A Tissue Propagation Model for Validating Close-Proximity Biomedical Radiometer Measurements

Q. Bonds, Member IEEE, P. Herzig and T. Weller, Senior Member IEEE

***Abstract*— The propagation of thermally-generated electromagnetic emissions through stratified human tissue is studied herein using a non-coherent mathematical model. The model is developed to complement subsurface body temperature measurements performed using a close proximity microwave radiometer. The model takes into account losses and reflections as thermal emissions propagate through the body, before being emitted at the skin surface. The derivation is presented in four stages and applied to the human core phantom, a physical representation of a stomach volume of skin, muscle, and blood-fatty tissue. A drop in core body temperature is simulated via the human core phantom and the response of the propagation model is correlated to the radiometric measurement. The results are comparable, with differences on the order of 1.5 – 3%. Hence the plausibility of core body temperature extraction via close proximity radiometry is demonstrated, given that the electromagnetic characteristics of the stratified tissue layers are known.**

***Index Terms*— Radiative Transfer, Biomedical Radiometric Sensing, Non-Contact Biomedical Sensing, Close Proximity Health Monitoring, Near Field Biomedical Sensing, Non-Invasive Biomedical Monitoring.**

I. Introduction

The work described herein explores the feasibility of core body temperature determination, via close proximity microwave radiometry and an associated tissue propagation model, for use as a health monitoring aid. The intended application is a wearable radiometric sensor deployable inside an astronaut extra vehicular suit (EVA), protective clothing worn by firefighters and other rescue personnel, or uniforms worn by soldiers. The sensor is designed to operate within the L-band frequency range of 1 GHz – 2 GHz, a spectrum which permits sufficient detection of emissions from regions below the skin surface. The theoretical detection depth is up to 30 mm, enabling thermographic measurements through layers of skin, fat, and muscle tissue [1] - [3]; as a result, the extraction of core body temperature is plausible with proper positioning of the sensor.

Manuscript received December 10, 2013. This work was supported by the National Science Foundation (#ECS-0901779), NASA, and Raytheon. The authors are indebted to Dr. John Gerig for his assistance in radiometer development.

Q. Bonds is currently with NASA Goddard, however the work was performed as a PhD candidate at the University of South Florida, Tampa, FL 33620 USA (phone: 334-233-9980; e-mail: qbonds@mail.usf.edu).

T. Weller is with the University of South Florida, Tampa, FL 33620 USA (phone: 813-974-2740; fax: 813-924-5250; e-mail: weller@usf.edu).

P. Herzig., is with Raytheon, Largo, FL 33777 USA. (Paul_A_Herzig@raytheon.com)

As discussed in previous studies, e.g. [4], the radiometric measurement is greatly influenced by the stratified dielectric layering of the human body. As electromagnetic waves propagate through the body, a portion of the power is dissipated due to the lossy nature of the tissue. This propagating energy is further attenuated by dielectric mismatch which gives rise to reflections at the tissue boundaries. As a result of these propagation effects, thermal emissions radiated from deep within the body have only a marginal effect on the brightness temperature emitted at the skin surface. It has been shown, for example, that thermal variations on the order of ±7 ºF from homeostasis will only result in a ±1 ºF change in skin temperature [5]. In consideration of such findings, the need for a non-invasive core body measurement method becomes apparent.

In [6], subcutaneous temperature variations of a human core phantom (HCP) were tracked using a microwave radiometer without considering a priori knowledge of the electrical properties of the internal tissue, i.e., muscle, blood and fat; only the dielectric properties of the skin surface were considered in the analysis. After applying a non-contact model (NCM) to account for certain close-proximity effects a difference of 1.2% – 8% was observed between the physical temperatures measured internally using thermal probes and the extracted radiometric brightness temperatures [7]. Though the results were promising, the methodology did not enable the physical temperature of the core to be predicted from the composite brightness temperature measured at the surface. These preliminary studies were performed for demonstration of the concept, thereby establishing a baseline for the method prior to considering the propagation effects of the tissue.

This study introduces a new tissue propagation model which provides an important advancement toward direct correlation between emitted brightness temperature and internal body temperature. The primary goal of the model, derived in Section II, is to characterize radiative transfer through the body while taking into account losses and reflections throughout the stratified tissue. The human core phantom, radiometric sensor and experimental validation of the model are described in Section III. This work demonstrates that core body temperature can be determined within about 3% error using the tissue propagation model, but requires additional knowledge of the intervening tissue layers. This knowledge cannot be accounted for by the radiometric measurement alone, and a method for determining these parameters is briefly discussed.

II. Derivation of the Tissue Propagation Model (TPM)

The tissue propagation model (TPM) characterizes radiative transfer through three tissue layers of an abdominal cavity compromised of skin, muscle, and blood-fatty tissue. Accordingly, the TPM derivation is applied to the human core phantom (HCP), with the tissue defined as stratified lossy dielectrics. Coherent transmission effects are not significant due to the lossy nature of the tissue layers, and are therefore ignored in the TPM; this simplification is validated by

comparison of the TPM to a coherent model in Section III. Angular dependence and scattering at the air-skin interface are also ignored since scattering at this boundary will be negligible. This interface is spatially homogeneous, given that the wavelength of the sensing frequency of 1.4 GHz (λ = 214 mm) is much larger than the roughness of the tissue under investigation (TUI) [8]; the condition applies here, as keratinocyte skin cells possess size and roughness on the order of micrometers. It has also been proven that the angular dependence is negligible in media with a high dielectric constant such as human tissue, since the polarization of the waves emanating from the tissue will remain relatively parallel to the respective boundary or transmission interface. The radiated energy is expected to be aligned with the observation angle of the sensor, assuming the device remains parallel with the TUI.

The TPM derivation is based on Ulaby's formulation for apparent brightness temperature of a terrain with a non-uniform dielectric profile [8]. These equations have been correlated to the physical makeup of the HCP, except the reflection at the muscle/blood boundary is ignored since the dielectric contrast between muscle and blood-fatty tissue layers is marginal, resulting in minimal reflections.

The TPM derivation is implemented in four levels:

1) Individual Stratum Emissions, $T_{s.t}$
2) Up and Down-Welling Emissions per Layer, $T_{t.U}$ and $T_{t.D}$
3) Net Apparent Stratum Emissions, T_B
4) Apparent Brightness Temperature Emitted at the Skin Surface, $T_{B.AP}$

A graphical representation of the TPM is presented in Fig. 1.

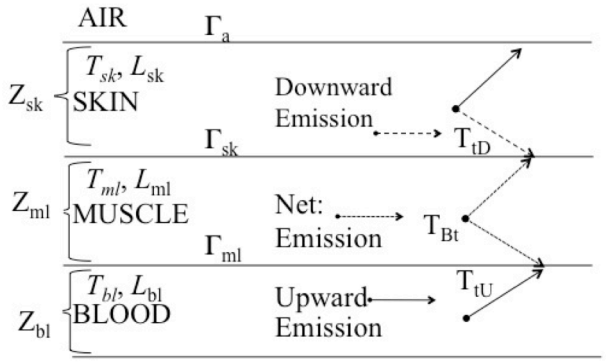

Fig. 1 Graphical representation of the tissue propagation model (TPM).

A. Stage 1: Individual Stratum Emissions

To begin, the stratum temperatures $T_{s,t}$ are defined, which are the total transmitted emissions, before reflection, at each tissue layer t: t = a (air), t = sk (skin), t = ml (muscle), and t = bl (blood). The expressions for $T_{s,t}$ are provided in (1) – (3), where L_t is the loss in the tissue, and T_t is the physical temperature of the stratum. As illustrated in Fig. 1, T_{bl} acts as an infinite source at the tissue boundary, and therefore does not carry a loss contribution. The equation for the loss contributions in the skin and muscle strata is presented in (4) where α_t is the attenuation constant (5), Z_t is the thickness of the tissue layer, $\varepsilon_{r,t}''$ is the imaginary part of the relative dielectric constant and $\varepsilon_{r,t}'$ the real part of the relative dielectric constant per layer. Finally, Γ_t is the power reflection coefficient at the tissue boundary, which is a function of the dielectric mismatch between the tissue layers (6).

$$T_{s.bl} = T_{bl} \tag{1}$$

$$T_{s.ml} = T_{ml}\left(1 - \frac{1}{L_{ml}}\right) \tag{2}$$

$$T_{s.sk} = T_{sk}\left(1 - \frac{1}{L_{sk}}\right) \tag{3}$$

$$L_t = e^{\alpha_t Z_t} \tag{4}$$

$$\alpha = \omega\sqrt{\left[\frac{\mu\varepsilon_{r,t}'\varepsilon_0}{2}\left(\sqrt{1+\left(\frac{\varepsilon_{r,t}''}{\varepsilon_{r,t}'}\right)^2}\right)-1\right]} \tag{5}$$

$$\Gamma_t = \left|\frac{\sqrt{\varepsilon_{r,t}'} - \sqrt{\varepsilon_{r,t}''}}{\sqrt{\varepsilon_{r,t}'} + \sqrt{\varepsilon_{r,t}''}}\right|^2 \tag{6}$$

B. Up- and Down-Welling Emissions

To derive an expression for the up- and down-welling contributions per layer, a similar procedure is followed to that of [8], wherein a binomial expansion $(1-\chi)^{-1}$ is formed from an expression which takes into account all reflections and losses throughout the stratified tissue. The formula for χ is presented in (7). In this case, χ accounts for losses and reflections between the air/skin and skin/muscle boundaries, while ignoring the negligible reflections at the muscle/blood boundary. The closed form of the binomial series is multiplied by an additional factor of $(1-\Gamma_a)$ to account for transmission at the air/skin interface. This closed form expression is defined as the coefficient of multiple reflections (CMR) in (8). The CMR is used in the derivation of the individual up- and/or down-welling temperature contributions in each layer. Thus, the up-welling contribution for the blood-fatty tissue layer is presented in (9), while the up- and down-welling contributions for the muscle are defined in (10) – (11) and for skin in (12) – (13).

$$\chi = \frac{\Gamma_{ml}\Gamma_a}{\left(L_{ml}L_{sk}\right)^2} \tag{7}$$

$$CMR = \frac{(1-\Gamma_a)}{1-(\chi)} \tag{8}$$

$$T_{bl.U} = T_{s.bl}\left(\frac{1-\Gamma_{ml}}{L_{ml}L_{sk}}\right)\left[CMR\right] \tag{9}$$

$$T_{ml.U} = \left(\frac{T_{s.ml}}{L_{sk}}\right)\left[CMR\right] \tag{10}$$

$$T_{ml.D} = T_{s.ml}\left(\frac{\Gamma_{ml}}{L_{ml}{}^{2}L_{sk}}\right)\left[CMR\right] \quad (11)$$

$$T_{sk.U} = T_{s.sk}\left(1-\frac{1}{L_{sk}}\right)\left[CMR\right] \quad (12)$$

$$T_{sk.D} = T_{s.sk}\left(\frac{\Gamma_{ml}}{L_{ml}{}^{2}L_{sk}}\right)\left[CMR\right] \quad (13)$$

C. Net Apparent Stratum Emissions

The net apparent brightness emissions from all strata (T_B) are comprised of the up- and/or down-welling emissions per layer, while taking all reflections into account. The total up- and down-welling contributions for each individual layer are represented by $T_{B.t}$ in (14) – (16). Due to its assumed infinite thickness the radiating source, $T_{bl.U}$ contributes only as an up-welling temperature (14). Infinite thickness is assumed in $T_{B.bl}$ since the depth of the blood-fatty tissue layer goes beyond that of the sensor detection depth (δ = ~30 mm). $T_{B.ml}$ and $T_{B.sk}$ are comprised of up-welling emissions T_{tU} (solid lines in Fig. 1), as well as down-welling emissions T_{tD} (dashed lines in Fig. 1). These expressions are provided in (15) – (16).

$$T_{B.bl} = T_{bl.U} \quad (14)$$

$$T_{B.ml} = T_{ml.U} + T_{ml.D} \quad (15)$$

$$T_{B.sk} = T_{sk.U} + T_{sk.D} \quad (16)$$

Hence, T_B is the sum of the net apparent emissions from all three layers (17)

$$T_B = T_{B.bl} + T_{B.sk} + T_{B.ml} \quad (17)$$

D. Apparent Brightness Emissions, $T_{B.AP}$

The remaining step is to formulate an expression for the net apparent brightness temperature emitted at the skin surface, $T_{B.AP}$. $T_{B.AP}$ takes into account T_B, the net brightness contributions from all strata (17), as well as the down-welling ambient temperature T_{dn}. As described in [7], T_{DN} is T_{dn} after being attenuated by multiple reflections and losses in the tissue layers. By assuming thermal equilibrium, i.e. $T_{sk} = T_{ml} = T_{DN}$, T_{DN} can be equated to T_B to resolve a second coefficient of multiple reflections denoted by CMR2 (18), yielding (19).

$$CMR2 = \frac{(1-2\Gamma_a)\left(\frac{\Gamma_{ml}}{L_{ml}L_{sk}}+\Gamma_a\right)}{1-(\chi)} \quad (18)$$

$$T_{DN} = T_{dn}CMR2 \quad (19)$$

The final expression for $T_{B.AP}$ is presented in (20).

$$T_{B.AP} = T_B + T_{DN} \quad (20)$$

III. EXPERIMENTAL VALIDATION

The measurement test bed used in this work is a human core phantom (HCP) developed to mimic the electromagnetic characteristics of a human core, assuming a constant blood flow rate. The total depth of the HCP is 50 mm, with diameters of 50 mm and 75 mm at d = 50 mm and d = 0 mm, respectively. As illustrated in

Fig. 2, this volume ideally captures the antenna-sensor main probing region incident to an abdominal cavity, and therefore takes the form of a Gaussian contour. As described in [7], the ability of the HCP to accurately emulate a human core is demonstrated by comparing the dielectric properties of the skin, muscle, and blood-fatty tissue phantoms to the Gabriel model which is generally accepted as the gold standard for human tissue characterization [9]. The skin-muscle phantom was developed in-house at the USF WAMI Center, and the details of the blood phantom recipe can be found in [10]. The radiometric sensor consists of a cavity backed slot antenna (CBSA), RF front end, and I/Q channels with an integrated rms detector [7]. It is important to note that the CBSA is critical to the overall functionality of the sensor, as it has been designed for optimal performance in close proximity to biological media; the details of the design are presented in [11].

Close-proximity brightness temperature measurements were performed using the radiometer and compared to the net apparent brightness temperature emitted at the skin surface ($T_{B.AP}$), as predicted by the tissue propagation model. The radiometer measurement data is post-processed using a non-contact model (NCM) which yields the brightness temperature emitted from all strata, extracted just below the surface of the skin. Hereafter, the latter will be denoted by MRBS. The NCM takes into account artifacts which arise due to the close positioning of the antenna to the specimen; details of NCM derivation are presented in [7]. In the final analysis, the results of the tissue propagation model (TPM) are compared to the post-processed MRBS data to determine the degree of correlation between the two data sets.

A. Measurement Technique

In an effort to mimic a drop in core body temperature (T_C), the blood-fatty tissue phantom was allowed to cool for 30 minutes after being heated to $T_C \geq 111$ °F in a separate glass container. A data logger thermometer was used to monitor the physical temperatures of the phantom layers as the brightness temperature was tracked across the depth using the radiometer. As illustrated in

Fig. 2, the physical temperature of the skin phantom was measured using a thermocouple placed on its surface. The muscle phantom temperature was measured using a thermocouple inserted into the center of the phantom. Finally, the inner core was tracked using an average temperature from three evenly spaced internal thermocouples positioned at a depth of ~42 mm beneath the skin layer, which is approximately 35 mm beneath the muscle layer. The temperatures of the skin and muscle phantom layers were near ambient, while the temperature of the inner core varies outside the dynamic range of the body (107 °F to 93 °F).

B. Applying the TPM

Application of the TPM to calculate the net apparent

brightness temperature emitted at the skin surface requires values for the electrical properties (α_t, L_t) and physical characteristics (T_t, Z_t) of the tissue layers, where α_t is the attenuation constant of layer t, L_t is the loss, T_t is the temperature, and Z_t the thickness. The values for Z_t, Γ_t, α_t and L_t are provided in Table 1.

Table 1. Calculated values of α_t, Z_t, Γ_t and L_t.

LAYER	Z (mm)	Γ	α (Np m^{-1})	L (Np)
BLOOD	40.0	0.00	34.70	19.45
MUSCLE	8.00	0.01	41.60	1.95
SKIN	2.00	0.56	37.10	1.18

C. *Analysis of the Data*

The comparison of the emitted brightness temperature calculated from the TPM, $T_{B.AP}$, to the post-processed brightness temperature detected by the radiometer, MRBS, is given in Fig. 3 and 4. The coherent Wilheit model is also used in the comparison to show that phase-dependent scattering can indeed be ignored [8], [12]. The differences between the TPM, MRBS, and Wilheit data are on the order of 1.5% – 3%. This correlation is impressive given that the MRBS measurement is quite sensitive to many close proximity effects. For instance, [7] demonstrates that a 1 degree inaccuracy in ambient temperature could yield error values on the order of 10% – 15%, which is equivalent to 10 ºF – 15 ºF. [7] also demonstrates that the post-processed MRBS results are very sensitive to the value assumed for the antenna impedance match.

Ultimately, core temperature extraction is plausible by solving for T_{bl} in the $T_{B.AP}$ expression, yielding (21), where MRBS has been substituted for $T_{B.AP}$. α_t, L_t, and Γ_t are calculated from (4) – (5), as a function of Z_t. In practice Z_t can be estimated based on the body fat percentage, weight, and height of the individual using bioelectrical impedance analysis. The remaining unknowns are $T_{sk} \in T_{B.sk}$ and $T_{ml} \in T_{B.ml}$, the physical temperatures of the skin, and muscle, respectively.

$$T_{bl} = \left(\frac{L_{ml}L_{sk}}{1-\Gamma_{ml}}\right)\left(\frac{(T_{B.AP} \cong MRBS) - T_{B.sk} - T_{B.ml} - T_{DN}}{CMR}\right) \quad (21)$$

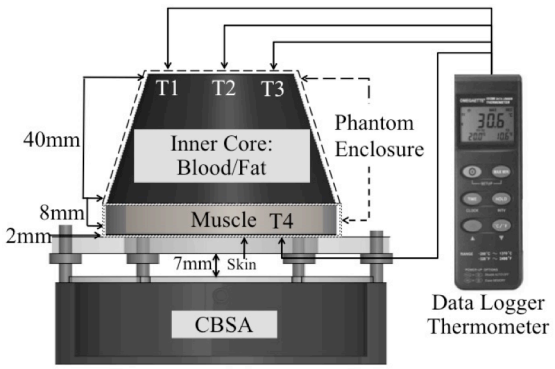

Fig. 3 Measurement test bed.

T_{sk} is typically a measurable quantity that can be determined by an infrared thermometer. T_{ml} is resolved by applying a heat transfer difference equation at the skin/muscle boundary to express the heat transfer profile of T_{ml} as a function of T_{sk} and other known heat transfer constants of the body [2].

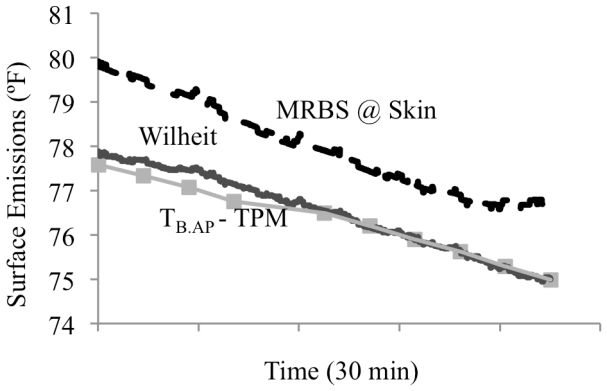

Fig. 2 Emitted brightness temperature at the surface (Skin) of the HCP, measured by the radiometer (MRBS) and compared to the TPM output, $T_{B.AP}$ and Wilheit model.

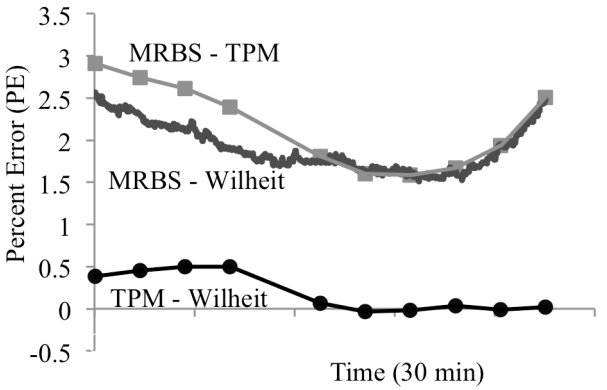

Fig. 4 Percent difference plots: MRBS – TPM, MRBS – Wilheit, Model and Wilheit – TPM.

IV. CONCLUSION

The tissue propagation model (TPM) presented herein is a important component for subsurface body temperature extraction using microwave radiometry. The four level derivation is based on a similar procedure employed in [8] for net apparent brightness temperature of a stratified dielectric media. The TPM is applied to a human core phantom and the results were compared to that of the close-proximity measurement taken with the radiometer. The results were promising, yielding marginal differences on the order of 1.5% - 3%. Such promising results demonstrate that the extraction of core body temperature can be achieved with high accuracy by implementing mathematical models to complement the radiometric measurement. However, to validate the current methodology as a practical health monitoring device, supporting research is needed in the area of bioelectrical impedance analysis and heat transfer theory, to resolve

unknowns not accounted for in the radiometric measurement.

REFERENCES

[1] L.R. Ballew, "A Microwave Radiometer for use in Biomedical Sensing Applications," Master's Thesis, Baylor University, 2006

[2] F, Bardati, and S. Iudicello, "Modeling the Visibility of Breast Malignancy by a Microwave Radiometer," *IEEE Transactions on Biomedical Engineering*, vol. 55, pp. 214-221, January 2008.

[3] A.T. Oikonomou, I.S. Karanasiou, and N.K.Uzunoglu "Phased-Array Near Field Radiometry For Brain Intracranial Applications," *Progress In Electromagnetics Research*, vol. 109, pp. 345–360, 2010

[4] M.S. Hawley, J. Conway, A.P. Anderson, and P.A. Cudd, "The influence of tissue layering on microwave thermographic measurements," *International Journal of Hyperthermia*, vol. 4, no. 4, pp. 427-435, July 1988

[5] O. Jay, F.D. Reardon, P. Webb, M.B. Ducharme, T. Ramsa, L. Nettlefold, and G.P. Kenny, "Estimating changes in mean body temperature for humans during exercise using core and skin temperatures is inaccurate even with a correction factor," *Journal of Applied Physics*, vol., pp. 443–451, 2007

[6] Q. Bonds, T. Weller, B. Roeder and P. Herzig, "A Total Power Radiometer (TPR) and Measurement Test Bed for Non Contact Biomedical Sensing Applications," *IEEE Wireless and Microwave Technology Conference*, 2009

[7] Q. Bonds, J. Gerig, T. Weller, and B. Roeder, "Towards Core Body Temperature Measurement via Close Proximity Radiometric Sensing," *IEEE Sensors Journal, Special Issue on Non-Invasive Physiological Monitoring*, **publication date**; **June 2011**

[8] F.L. Ulaby, R.K. Moore, and A.K. Fung, Microwave Remote Sensing, Active and Passive, vol 1, pp. 236-244, Artech House, 1981

[9] C. Gabriel, and S. Gabriel, "Compilation of the Dielectric Properties of Body Tissues at RF and Microwave Frequencies," Brooks AFB report number AL/OE-TR-1996-0037, 1996

[10] Australian Communication Authority, "Radiocommunications (Electromagnetic Radiation Human Exposure) Standard 2003," Radio Communications Act, 1992 Section 162, June 2003

[11] Q. Bonds, T. Weller, B. Roeder and P. Herzig, "A tunable Cavity Backed Slot Antenna (CBSA) for close proximity biomedical sensing applications," *in IEEE Microwaves, Communications, Antennas and Electronics Systems*, 2009

[12] T. T. Wilheit, "Radiative transfer in a plane stratified dielectric," *IEEE Transactions on Geoscience and Remote Sensing*, vol. 16, pp. 138-143, 1978

[13] T. Togawa, " Body Temperature Measurement," *The Journal of Clinical Physical Physiology Measurements,* vol. 6, pp. 83-108, 1985

[14] Y. Kurazumi, T. Tsuchikawa, J. Ishii, K. Fukagawa, Y. Yamato, N. Matsubara, "Radiative and convective heat transfer coefficients of the human body in natural convection," *The Journal of Building and Environment,* vol. 43, pp. 2142-2153, 2008

Quenton Bonds (M'2004) received the B.S. degree in Mathematics from Alabama State University in Montgomery Alabama in 2001 and the M.S. degree in Electrical Engineering in 2006 from The University of South Florida (USF) in Tampa Florida and went on to attain the Ph.D. from USF in 2010. Dr. Bonds is currently a research electronics engineer in the Microwave Instruments and Technology Branch of the National Aeronautics and Space Administration (NASA) at the Goddard Space Flight Center (GSFC) in Greenbelt Maryland. His current research focus can be generally characterized within the design and development of remote sensors for Geoscience and space applications. In particular, he is very involved in the research and development of novel antennas for SAR and other radar applications, as well as, radiometric sensor design and calibration.

Paul A. Herzig has over 35 years professional experience at Raytheon in the design and test of RF, microwave and millimeter wave components and systems for communications, including space, airborne, ship-board, and ground-based applications, and passive and active remote sensing, including space and human body sensing. He currently holds 1 patent, has two patents pending and has authored or co-authored a number of papers on a variety of topics including high power UHF filter design for space application, remote sensing and metamaterials based antennas. Mr Herzig's current research interests involve applications of metamaterials to GPS and conformal antennas and RF filters.

Thomas M. Weller (S'92-M'95-SM'98) received the B.S., M.S. and Ph.D. degrees in Electrical Engineering in 1988, 1991, and 1995, respectively, from the University of Michigan, Ann Arbor. From 1988-1990 he worked at Hughes Aircraft Company in El Segundo, CA. He joined the University of South Florida in 1995 where he is currently a professor and chair in the Electrical Engineering Department. He co-founded Modelithics, Inc. in 2001. Dr. Weller was a recipient of the Outstanding Young Engineer Award from the IEEE Microwave Theory and Techniques Society in 2005, the USF President's Award for Faculty Excellence in 2003, IBM Faculty Partnership Awards in 2000/2001, a National Science Foundation CAREER Award in 1999 and the IEEE MTT Society Microwave Prize in 1996. His current research interests are in the areas of RF micro electromechanical systems, development and application of microwave materials, and integrated circuit and antenna design. He has 21 U.S. patents and over 200 professional journal and conference publications.